



**HAL**  
open science

# Ab initio Raman spectrum of the normal and disordered Mg Al<sub>2</sub> O<sub>4</sub> spinel

Michele Lazzeri, Pascal Thibaudeau

## ► To cite this version:

Michele Lazzeri, Pascal Thibaudeau. Ab initio Raman spectrum of the normal and disordered Mg Al<sub>2</sub> O<sub>4</sub> spinel. *Physical Review B: Condensed Matter and Materials Physics* (1998-2015), 2006, 74, pp.140301(R). 10.1103/PhysRevB.74.140301 . hal-00130125

**HAL Id: hal-00130125**

**<https://hal.science/hal-00130125>**

Submitted on 7 Oct 2023

**HAL** is a multi-disciplinary open access archive for the deposit and dissemination of scientific research documents, whether they are published or not. The documents may come from teaching and research institutions in France or abroad, or from public or private research centers.

L'archive ouverte pluridisciplinaire **HAL**, est destinée au dépôt et à la diffusion de documents scientifiques de niveau recherche, publiés ou non, émanant des établissements d'enseignement et de recherche français ou étrangers, des laboratoires publics ou privés.

***Ab initio* Raman spectrum of the normal and disordered MgAl<sub>2</sub>O<sub>4</sub> spinel**

Michele Lazzeri

*IMPMC, Universit s Paris 6 et 7, CNRS, IPGP, 140 rue de Lourmel, 75015 Paris, France*

Pascal Thibaudeau

*Commissariat   l'Energie Atomique, Le Ripault, Bo te Postale 16, 37260 Monts, France*

(Received 2 June 2006; revised manuscript received 9 October 2006; published 31 October 2006)

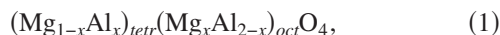
*Ab initio* calculations, based on density functional theory, of the vibrational Raman spectra of both normal and cationic disordered MgAl<sub>2</sub>O<sub>4</sub> spinel are reported. The vibrational properties of the disordered system are obtained in two steps. First, the interatomic force constants of small defective supercells are computed in a fully *ab initio* way. Later, these force constants are used to build the dynamical matrices of larger disordered systems. The calculated Raman spectrum presents the mode near 727 cm<sup>-1</sup> which is due to the presence of cationic disorder and which is commonly attributed to a breathing mode (BM) of AlO<sub>4</sub> tetrahedra. Contrary to previous interpretations, the 727 cm<sup>-1</sup> mode is due to phonons which are silent in the perfect crystal and become Raman active in the disordered structure because of the coupling with the BM of the MgO<sub>4</sub> tetrahedra.

DOI: 10.1103/PhysRevB.74.140301

PACS number(s): 78.30.Ly, 91.60.Mk, 71.15.Mb

MgAl<sub>2</sub>O<sub>4</sub> spinel is often considered as the prototype of a large class of solid oxides of geological and technological interest.<sup>1</sup> For instance, the spinel transition of olivine, which is the major constituent of the Earth's mantle, is widely accepted to be the origin of the 410 km seismic discontinuity.<sup>2</sup> Moreover, spinel oxides are found to be highly resistant to radiation-induced swelling and transformations at elevated temperatures.<sup>3,4</sup> Because of this, they are favorably considered in the next generation of nuclear power plant design. The generic formula of the minerals that crystallize in the II-III spinel structure is AB<sub>2</sub>O<sub>4</sub>, where *A* is a divalent cation and *B* is a trivalent cation. The oxygen atoms belong to a close-packed pseudo-face-centered cubic sublattice. In a so-called normal arrangement, all the divalent cations are at the center of a tetrahedral site (coordinated with four oxygen atoms), while the trivalent cations are at the center of an octahedral site (coordinated with six oxygen atoms).

The study of these systems is complicated by order-disorder phenomena. Particularly in MgAl<sub>2</sub>O<sub>4</sub>, an exchange is observed between the two types of cations in tetrahedral and octahedral sites, which gives rise to partially inverse spinel. Such changes in cationic order, usually induced by high temperature and/or high pressure, can be characterized by the formula



where it is indicated that some Al atoms in the structure have switched with some Mg atoms from the octahedral to the tetrahedral sites at a *x* rate. There are many experimental methods to characterize the degree of disorder in such systems and most of the experimental studies on spinels deal with the determination of *x* with respect to temperature and/or pressure. Electron spin resonance<sup>5</sup> on a natural MgAl<sub>2</sub>O<sub>4</sub> spinel for temperature lower than 1278 K and high-resolution <sup>27</sup>Al nuclear magnetic resonance on quenched natural or synthetic samples<sup>6-8</sup> have been intensively used. Other techniques, such as neutron<sup>9,10</sup> and x-ray diffraction,<sup>11,12</sup> have been reported. In this context, it would be interesting to know whether Raman spectroscopy<sup>13,14</sup> can

be used as well. The first step toward this direction is to make a proper assignments of the vibrational modes.

The proper assignments of the vibrational modes in the spinel is a long-standing problem (see Ref. 15 for a review). An important difficulty is the well-known fact that spectra of different samples are qualitatively different. This is true also for samples which are supposed to have the same chemical composition. In particular, in the spectra of natural spinel, above 600 cm<sup>-1</sup>, there are usually only two peaks at ~670 and ~770 cm<sup>-1</sup>. On the contrary, an additional well-defined peak is observed at 727 cm<sup>-1</sup> in synthetic spinels. The first clear demonstration that the 727 cm<sup>-1</sup> is related to the presence of structural disorder (and not, e.g., to the presence of chemical impurities or to a combination of harmonic modes) was given by Cynn *et al.* in Ref. 4. It is commonly assumed that the 770 cm<sup>-1</sup> mode is due to the symmetric stretching of the MgO bonds in the MgO<sub>4</sub>, which here we call the tetrahedral breathing mode (TBM). By using a polarized laser, Cynn *et al.* observe that the 727 cm<sup>-1</sup> peak has the same symmetry as the 770 cm<sup>-1</sup> peak and, tentatively, attribute this peak to the TBM of AlO<sub>4</sub> (Al-TBM), following Refs. 15-17. Later, de Wijs *et al.*<sup>18</sup> calculated using *ab initio* methods<sup>19</sup> the vibrational properties of MgAl<sub>2</sub>O<sub>4</sub> finding that the presence of an AlO<sub>4</sub> tetrahedron in the spinel is, indeed, associated with two Al-TBMs at 723 and 757 cm<sup>-1</sup>. However, these authors did not perform a Raman-intensity calculation which could definitely confirm the attribution of the 727 cm<sup>-1</sup> mode to Al-TBM.

In this paper, the Raman spectrum of MgAl<sub>2</sub>O<sub>4</sub> spinel is computed using density functional theory<sup>19</sup> (DFT) for both the perfect and of the partially inversed crystals.

In an insulating crystal, the frequency and the intensity of the Raman peaks are determined by the zone-center phonon frequencies and by the Raman tensor.<sup>20</sup> The phonon frequencies are determined by the dynamical matrix, dielectric constant, and Born effective charges,<sup>21,22</sup> which are obtained using the DFT-based approach of Ref. 21. Calculations are done with the PWSCF code<sup>23</sup> using norm-conserving pseudo-potentials and plane waves (80 Ry cutoff) methods. Electronic integration is performed on a 4 × 4 × 4 *k*-point grid for

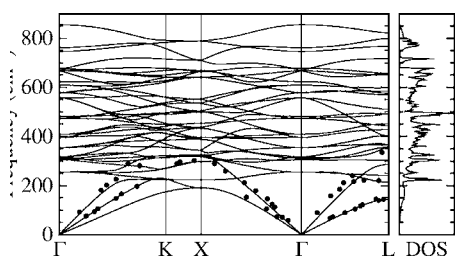


FIG. 1.  $\text{MgAl}_2\text{O}_4$  spinel phonon dispersion from DFT calculation. Dots are measurements from Ref. 24. Right panel: Phonon density of states.

the bulk. Other details are the same as in Ref. 14. The bulk dynamical matrices are computed on a  $5 \times 5 \times 5$   $\mathbf{q}$ -point grid in a fully *ab initio* way. The Fourier transform of these dynamical matrices determines the interatomic force constants (IFCs) in real space, which, in turn, are used to obtain the phonon dispersion all over the Brillouin zone (Fig. 1), following the standard procedure. The dispersion of Fig. 1 is in good agreement with measurements<sup>24</sup> and previous DFT calculations.<sup>18</sup> Thus, following Ref. 25, the Raman tensor and the Raman spectrum are calculated (Fig. 2). The agreement with the measured spectrum of natural spinel is remarkable. Only five modes are Raman active<sup>4,18</sup> and the computed intensities reproduce quite well the measured one. The mode at  $557 \text{ cm}^{-1}$  is very weak and is not visible in the measurements. As expected, in the perfect  $\text{MgAl}_2\text{O}_4$  crystal there is not a Raman-active mode between  $667$  and  $762 \text{ cm}^{-1}$ , i.e., in correspondence with the  $727 \text{ cm}^{-1}$  peak observed in synthetic spinels. According to a direct analysis, the  $762 \text{ cm}^{-1}$

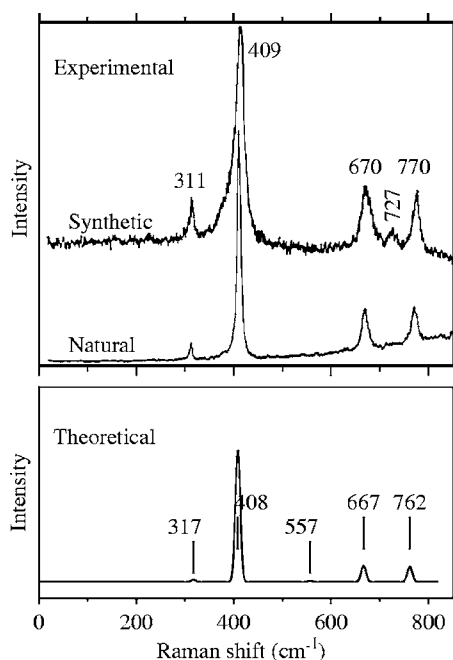


FIG. 2. Raman spectrum of  $\text{MgAl}_2\text{O}_4$  spinel. Upper panel: measurements from Ref. 4 on synthetic and natural spinel. Lower panel: DFT calculation on the perfect  $\text{MgAl}_2\text{O}_4$  crystal. The spectrum is convoluted with a uniform Gaussian broadening having  $5 \text{ cm}^{-1}$  width.

peak corresponds to a TBM of the oxygen atoms surrounding a Mg cation, thus confirming previous assignments.<sup>4</sup>

A partially inverse structure obtained by Mg-Al exchange is now considered. This system is a  $\text{MgAl}_2\text{O}_4$  crystal with a certain number of defects randomly distributed. Each defect corresponds to the exchange of a Mg atom with an Al atom. The fully *ab initio* computation of a large supercell with a big number of defects is not feasible, at present. However, if the vibrational properties are determined by the interaction among one defect and its nearest neighbors, a simpler approach is possible. One can compute the short-range IFCs on a small supercell with one defect and, later, use these IFCs to build the dynamical matrix of a larger disordered system. The method is similar to that commonly used to calculate the phonon dispersion of a crystal surface.<sup>26</sup>

Following this idea, a simple cubic supercell (56 atoms) with one defect is considered.<sup>27</sup> After the relaxation of the structure by energy and stress minimization, the *ab initio* dynamical matrix and the Raman tensor are computed. From this dynamical matrix, the IFCs between an Al atom on a tetrahedral site and its four neighboring O atoms are determined. The calculation is repeated putting the defect in different positions in the cubic 56-atom supercell, checking that, despite the distortion already reported in Ref. 18, the Al-O IFCs are slightly affected. In one case, a calculation with two defects<sup>27</sup> in the same supercell was also performed. According to our calculations, the presence of an Al cation in a tetrahedral site is associated with two Al-TBMs at  $\sim 720$  and  $\sim 750 \text{ cm}^{-1}$  in accordance with Ref. 18.

Then a  $4 \times 4 \times 4$  supercell is considered, whose IFCs are determined according to the IFCs previously calculated for the bulk. The Mg are exchanged with Al atoms in some of the tetrahedral sites randomly chosen and the IFCs of the five atoms concerned (and of the four Al-O couples) are substituted, for each defect, with the IFCs calculated for the defected supercell. The Raman tensor and the Born effective charges of the defected  $4 \times 4 \times 4$  supercell are obtained in an analogous way.<sup>28</sup> The dynamical matrix and the Raman tensor thus obtained can be used to calculate the Raman spectrum of the partially inverted structure. The phonon modes are obtained as usual by diagonalization of the dynamical matrix. This approach is in principle exact when the IFCs are short ranged and when the interaction between defects can be neglected (at low defect density for instance). Concerning the short-range character of the IFCs, in the present case the strongest IFCs between different atoms are those between nearest neighbors, decreasing to less than 5% for the other couples. Moreover, the strongest IFCs for a cation-anion couple is between Mg and O, decreasing to a value smaller than 35% for an Al-O couple. The present implementation is limited by the fact that only the change of the IFCs of the nearest neighbor O atoms around an Al are considered and by the use of a relatively modest  $4 \times 4 \times 4$  supercell. If a much larger supercell is required (and the diagonalization of the dynamical matrix is not feasible) an approach similar to that of Ref. 29 could be implemented.

In Fig. 3 the resulting Raman spectrum of a partially inverted structure [ $x=0.3$  in Eq. (1)] is shown. This particular choice of cationic rate is motivated by the fact that the extra Raman modes were observed after a rapid quench for a tem-

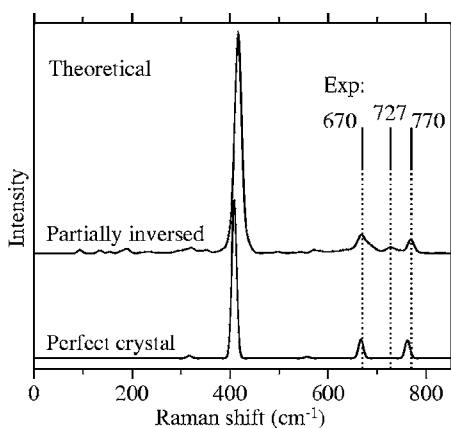


FIG. 3. Raman spectrum from DFT calculation on the perfect crystal and on a partially inversed structure [ $x=0.3$  in Eq. (1)]. The spectrum of the partially inversed structure is obtained from an average over several random configurations. The spectra are convoluted with a uniform Gaussian broadening having  $5 \text{ cm}^{-1}$  width.

perature higher than the critical order-disorder temperature where this rate is obtained.<sup>30</sup> A well-defined peak near  $727 \text{ cm}^{-1}$ , similar to the one observed in synthetic spinel, is clearly visible. Other small peaks present in the calculations at lower frequencies are an artifact of the calculation and depend on the supercell used.<sup>31</sup> It would be tempting to determine a relation between the intensity of the  $727 \text{ cm}^{-1}$  peak and the density of defects in the crystal, starting from Fig. 3. This relation could be later used to determine the defect density in a sample from its Raman spectrum. Unfortunately, at present, we cannot say whether the number extracted in this way is reasonable or not, given the simplified approach we are using (i.e., given the small number of defect IFCs considered). For the same reason, probably, the theoretical spectrum of Fig. 3 does not present the asymmetric widening of the main peak at  $490 \text{ cm}^{-1}$  that is found experimentally (compare the “synthetic” and “natural” spectra of Fig. 2). Finally, in the present approach the variation of the dynamical matrix due to the presence of some Mg in octahedral sites is not considered. This changes vibrations that are not Raman active.

An approach similar to that of Ref. 25 is now considered to determine the character of the vibrations of the  $727 \text{ cm}^{-1}$  mode. The spectrum of the partially inversed structure is projected on the TBM of the oxygen tetrahedra centered on Mg atoms (Mg-TBM) and of the oxygen tetrahedra centered on Al atoms (Al-TBM). The results are shown in Fig. 4. In Fig. 4, the corresponding overlap intensities (defined in p. 3, Sec. 3 of Ref. 25) are also reported. A Raman peak can be associated with a TBM (i.e., its Raman activity is due to a

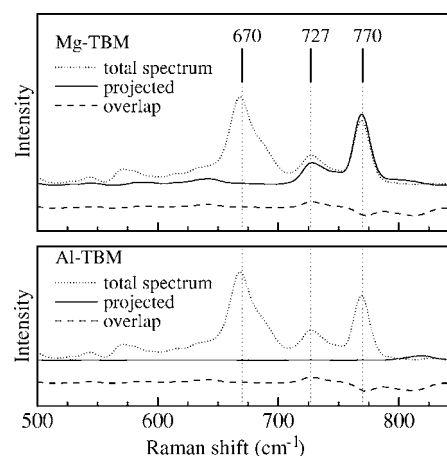


FIG. 4. Raman spectrum of the partially inversed structure of Fig. 3. The spectrum is projected on the in-phase breathing modes of the oxygen tetrahedra centered on the Mg (Al) atoms: Mg- (Al)-TBM, upper (lower) panel. The overlap intensity is shifted for clarity.

TBM) if and only if the overlap intensity is negligible compared to the projected intensity.<sup>25</sup> From Fig. 4 (upper panel), both peaks at  $727$  and  $770 \text{ cm}^{-1}$  are due to the Mg-TBM. In particular, according to a direct analysis of the vibrational modes, the  $727 \text{ cm}^{-1}$  mode is due to phonons that are silent in the perfect crystal and become Raman active in the disordered structure because of the coupling with the Mg-TBM. This result is counterintuitive and is in contradiction with the previous, tentative, attribution of the  $727 \text{ cm}^{-1}$  peak to the Al-TBM.<sup>4,18</sup> Moreover, the vibrations associated with the Al-TBM are not visible with Raman spectroscopy (lower panel of Fig. 4). This is due to the fact that the form of the Raman tensor associated with the oxygens of the Al tetrahedra is very different from the one associated with the oxygens of the Mg tetrahedra and the Raman tensor component of the Al-TBM vibrations is smaller compared to the one of the Mg-TBM.<sup>32</sup>

Concluding, the Raman spectrum of the partially inversed  $\text{MgAl}_2\text{O}_4$  spinel is determined using *ab initio* calculations based on DFT. We focused on the  $727 \text{ cm}^{-1}$  Raman peak, which is commonly attributed to the presence of cationic disorder and whose origin is debated.<sup>15</sup> Contrary to previous assignments, the  $727 \text{ cm}^{-1}$  mode is due to phonons that are silent in the perfect crystal and become Raman active in the disordered structure because of the coupling with the Mg-TBM.

Calculations were performed at IDRIS, Orsay (Grant No. 051202), and CEA, TERA-1 supercomputer.

<sup>1</sup>F. S. Galasso, *Structure and Properties of Inorganic Solids* (Pergamon, New York, 1970).

<sup>2</sup>A. E. Ringwood and A. Major, *Phys. Earth Planet. Inter.* **3**, 89 (1970).

<sup>3</sup>L. S. Cain, G. J. Pogatschnik, and Y. Chen, *Phys. Rev. B* **37**, 2645 (1988).

<sup>4</sup>H. Cynn, S. K. Sharma, T. F. Cooney, and M. Nicol, *Phys. Rev. B* **45**, 500 (1992).

- <sup>5</sup>U. Schmocker, H. R. Boesh, and F. Waldner, *Phys. Lett.* **40A**, 237 (1972).
- <sup>6</sup>B. J. Wood, R. J. Kirkpatrick, and B. Montez, *Am. Mineral.* **71**, 999 (1986).
- <sup>7</sup>R. L. Millard, R. C. Peterson, and B. K. Hunter, *Am. Mineral.* **77**, 42 (1992).
- <sup>8</sup>H. Maekawa, S. Kato, K. Kawamura, and T. Yokokawa, *Am. Mineral.* **82**, 1125 (1997).
- <sup>9</sup>R. C. Peterson, G. A. Lager, and R. L. Hitterman, *Am. Mineral.* **76**, 1455 (1991).
- <sup>10</sup>S. A. T. Redfern, R. J. Harrison, H. St. C. O'Neill, and D. R. R. Wood, *Am. Mineral.* **84**, 299 (1999).
- <sup>11</sup>T. Yamanaka and Y. Takeuchi, *Z. Kristallogr.* **165**, 65 (1983).
- <sup>12</sup>G. B. Andreozzi, F. Princivalle, H. Skogby, and A. Della Guista, *Am. Mineral.* **85**, 1164 (2000).
- <sup>13</sup>H. Cynn, O. L. Anderson, and M. Nicol, *Pure Appl. Geophys.* **141**, 415 (1993).
- <sup>14</sup>P. Thibaudeau and F. Gervais, *J. Phys.: Condens. Matter* **14**, 3543 (2002).
- <sup>15</sup>P. F. McMillan and A. M. Hofmeister, in *Spectroscopic Methods in Mineralogy and Geology*, edited by F. C. Hawthorne, Reviews in Mineralogy Vol. 18 (Mineralogical Society of America, Washington, DC, 1988), pp. 99–159.
- <sup>16</sup>L. M. Fraas, J. E. Moore, and J. B. Salzberg, *J. Chem. Phys.* **58**, 3585 (1973).
- <sup>17</sup>A. Chopelas and A. M. Hofmeister, *Phys. Chem. Miner.* **18**, 279 (1991).
- <sup>18</sup>G. A. de Wijs, C. M. Fang, G. Kresse, and G. de With, *Phys. Rev. B* **65**, 094305 (2002).
- <sup>19</sup>W. Kohn and L. J. Sham, *Phys. Rev.* **140**, A1133 (1965).
- <sup>20</sup>P. Brüesch, *Phonons: Theory and Experiments II* (Springer, Berlin, 1986).
- <sup>21</sup>S. Baroni, S. de Gironcoli, A. Dal Corso, and P. Giannozzi, *Rev. Mod. Phys.* **73**, 515 (2001).
- <sup>22</sup>X. Gonze and C. Lee, *Phys. Rev. B* **55**, 10355 (1997).
- <sup>23</sup>S. Baroni *et al.*, <http://www.pwscf.org/>
- <sup>24</sup>P. Thompson and N. W. Grimes, *Solid State Commun.* **25**, 609 (1978).
- <sup>25</sup>M. Lazzeri and F. Mauri, *Phys. Rev. Lett.* **90**, 036401 (2003); *Phys. Rev. B* **68**, 161101(R) (2003).
- <sup>26</sup>M. Lazzeri and S. de Gironcoli, *Surf. Sci.* **402-404**, 715 (1998); *Phys. Rev. Lett.* **81**, 2096 (1998).
- <sup>27</sup>The defect is obtained by exchanging a Mg atom with an Al atom. In this way, the stoichiometry of the defect cell is always equal to the one of the perfect  $\text{MgAl}_2\text{O}_4$  crystal. This is mandatory in order to preserve the insulating character of the system.
- <sup>28</sup>Although a detailed analysis is beyond the scope of the present work, we remark that, in the perfect crystal, the Born effective charges  $Z^*$  are 2.75, 2.02, and  $-1.88$  for Al, Mg, and O, respectively. These values are slightly affected by the cationic disorder. In particular,  $Z^*$  decreases by  $\sim 5\%$  for the Mg in the octahedral site, while it increases by  $\sim 3\%$  for the Al in the tetrahedral site. Concerning O atoms, the largest  $Z^*$  change is a reduction of  $\sim 5\%$  for the atoms in an Al tetrahedron.
- <sup>29</sup>N. Vast and S. Baroni, *Phys. Rev. B* **61**, 9387 (2000).
- <sup>30</sup>S. Da Rocha and P. Thibaudeau, *J. Phys.: Condens. Matter* **15**, 7103 (2003).
- <sup>31</sup>The disappearing of this artifact would be obtained by using a supercell much larger than the  $4 \times 4 \times 4$ , but this is presently not feasible. However, a clear indication of the nature of these peaks is obtained performing the calculation using supercells smaller than but different from the  $4 \times 4 \times 4$  of Fig. 3. The position and the presence of these peaks strongly depend on the supercell used. On the contrary, the peak near  $727 \text{ cm}^{-1}$  is always present and well defined and its position does not depend on the supercell.
- <sup>32</sup>The Raman intensity is given by the square of the Raman tensor, which is proportional to the derivative of the dielectric polarizability tensor with respect to an atomic displacement  $\partial \vec{\chi} / (\partial \tau)$ . Let us call  $\partial \vec{\chi} / (\partial u)$  the derivative of  $\vec{\chi}$  with respect to a displacement of the four oxygens surrounding a tetrahedron, toward the center of the tetrahedron, normalized to one per tetrahedron.  $\partial \text{Tr}(\vec{\chi}) / (\partial u)$  is  $0.13 (-0.06) \times (4\pi)^{-1}$  ( $\text{Bohr}^{-1}$ ) for a Mg (Al) tetrahedron, where “Tr” is the trace.